How does the molecular linker in dynamic force spectroscopy affect probing molecular interactions at the single-molecule level?



2016 Jpn. J. Appl. Phys. 55 08NB01

(http://iopscience.iop.org/1347-4065/55/8S1/08NB01)

Japanese Journal of Applied Physics **55**, 08NB01 (2016)
http://doi.org/**10.7567/JJAP.55.08NB01**

**REGULAR PAPER**

# How does the molecular linker in dynamic force spectroscopy affect probing molecular interactions at the single-molecule level?

Atsushi Taninaka, Kota Aizawa, Tatsuya Hanyu, Yuuichi Hirano, Osamu Takeuchi, and Hidemi Shigekawa

*Faculty of Pure and Applied Sciences, University of Tsukuba, Tsukuba, Ibaraki 305-8573, Japan*

Received October 6, 2015; accepted December 12, 2015; published online March 1, 2016

Dynamic force spectroscopy (DFS) based on atomic force microscopy, which enables us to obtain information on the interaction potential between molecules such as antigen–antibody complexes at the single-molecule level, is a key technique for advancing molecular science and technology. However, to ensure the reliability of DFS measurement, its basic mechanism must be well understood. We examined the effect of the molecular linker used to fix the target molecule to the atomic force microscope cantilever, i.e., the force direction during measurement, for the first time, which has not been discussed until now despite its importance. The effect on the lifetime and barrier position, which can be obtained by DFS, was found to be ~10 and ~50%, respectively, confirming the high potential of DFS. © 2016 The Japan Society of Applied Physics

## 1. Introduction

The understanding of molecular interactions in the formation of specific bonds based on reciprocal recognition is a key factor for understanding and utilizing the functions of molecules such as DNA and antigen–antibody complexes.[1–3] The probing of the interaction potential between two molecules is the basis for describing molecular reactions.[1–5] However, since functional molecules generally have complex structures, and local characteristics and reaction processes determine the observed molecular interactions, it is difficult to understand their functions from the results of conventional macroscopic analyses, which provide averaged information. Dynamic force spectroscopy (DFS) is a technique based on atomic force microscopy (AFM), which provides information on the interaction potential landscape between two molecules at the single-molecule level.[3,5–10] For example, since molecules such as streptavidin and avidin have multiple bonding sites, it is difficult to separately probe them in detail using conventional macroscopic methods which gives averaged value. In DFS, using the variation in the cross-linkers, selective analysis of the bonding sites has been realized, and direct and bridging interactions at each reaction site in a ligand–receptor system have been distinguished and individually analyzed.[8–11]

In DFS based on the Bell–Evans model,[4,12,13] the unbinding force applied to a pair of molecules is increased at a constant rate, and the force required to rupture the bond is measured. However, although the analysis is based on the assumption that the force is applied to a sample placed immediately below the probe tip [Fig. 1(a)], the molecular linker used to fix the target molecule to the cantilever may change the direction of the force [Fig. 1(b)]. Despite its importance, its effect on measurement has not been closely examined until now. To ensure the reliability of DFS measurement, it must be thoroughly understood and should be taken into account.

Here, we report the first results of simulations carried out to examine the effect of the direction of the force applied to a target molecule through a molecular linker.

## 2. Experimental procedure and theory

Figure 1 shows schematic illustrations of DFS measurement. As shown in Fig. 1(a), after forming a ligand–receptor structure, it is ruptured with the force applied by an atomic force microscope. In the DFS method, as described above, the unbinding force applied to a molecular bond is increased at a constant rate (loading rate $r$), and the force required to rupture the molecular bond is measured.[8,9] The modal rupture force $f^*$ is obtained as the most frequent rupture force of the histogram in the rupture force [right side in Fig. 1(a)].

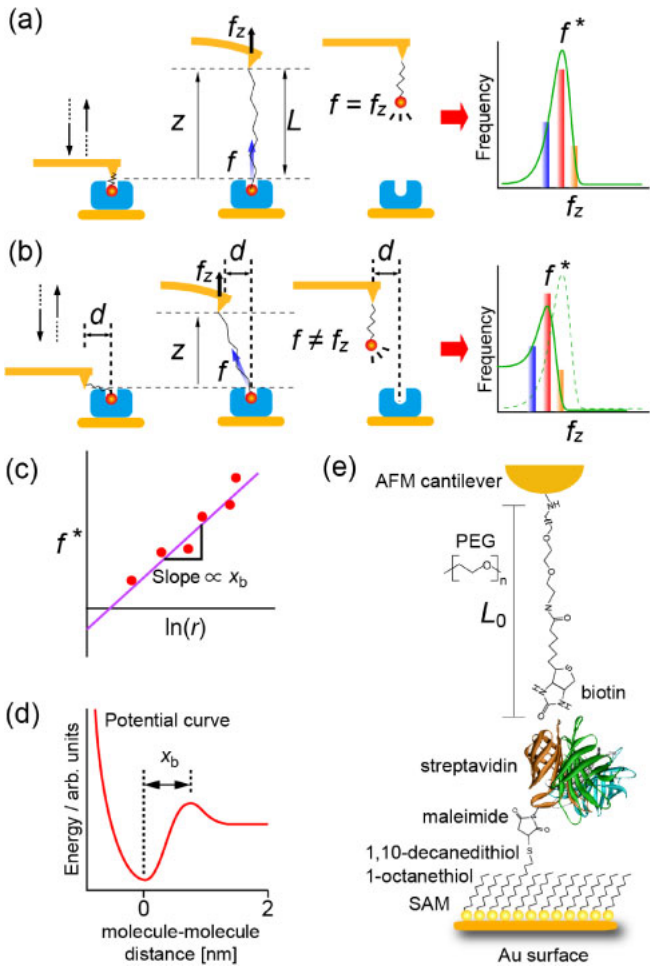


**Fig. 1.** (Color online) Schematic illustrations of DFS measurement for (a) $d = 0$ and (b) $d \neq 0$. (c) Relationship between modal rupture force $f^*$ and logarithm of loading rate $r$. The position of the barrier $x_b$ and the lifetime of the bond can be obtained from the slope and the intercept of the straight line, respectively. (d) Potential landscape of molecular interaction. $x_b$ indicates the position of the barrier. (e) Typical system with biotin (ligand)–streptavidin (receptor) used in DFS measurement. PEG: poly(ethylene glycol).

Figure 1(c) shows the relationship between $f^*$ and the logarithm of $r$. From the reciprocal value of the slope of the straight line and its intercept, the position of the potential barrier landscape $x_b$ [Fig. 1(d)] and the lifetime of the bond $\tau$ can be obtained.[4,7,9,11,12)]

When the molecular linker used to fix the molecule to the atomic force microscope tip is long, the coupling may be located at a distance $d$ below the atomic force probe as shown in Fig. 1(b). In this case, when the cantilever is pulled up, the force $f$ is applied obliquely to the target molecule, which results in a discrepancy in the rupture force measured by AFM as described above.

Figure 1(e) shows an illustration of a typical system with a biotin ligand and streptavidin receptor, which is widely used in this field[4–12,14,15)] and was adopted as a sample for the analysis in this work. Poly(ethylene glycol) (PEG) was used as a cross-linker molecule to reduce the effect of the probe on the measurement, i.e., steric barrier to hamper the natural bonding. Streptavidin was fixed using maleimide on a Au substrate covered with a film of 1-octanethiol and 1,10-decanedithiol (100 : 1) formed by self-assembly.

To analyze the behavior of a molecular linker, the wormlike chain (WLC) model has generally been adopted, which is particularly suitable for describing stiffer polymers with successive segments exhibiting cooperativity.[16–19)] In the WLC model, the energy of a molecular chain used as a cross-linker is described in terms of bending, twisting, and stretching. When the contribution of stretching is neglected and the molecular chain is sufficiently stiff to neglect a small extension, the energy of the molecular chain can be expressed in terms of the bending and extension energies that are generated when a force is applied to the end of the molecular chain.[16–19)]

Assuming the WLC model, the contractile force of PEG $f$ is written as

$$f = \left(\frac{k_B T}{A}\right)\left[\frac{1}{4(1 - L/L_0)^2} - \frac{1}{4} + \frac{L}{L_0}\right], \tag{1}$$

where $A$ is the persistence length,[20)] $L_0$ is the contour length (molecular length), $L = \sqrt{z^2 + d^2}$ is the extension length of the molecule, $k_B$ is the Boltzmann constant, and $T$ is the temperature, and $z$ is the retraction distance of the probe-tip apex shown in Fig. 1. The persistence length is the scale used to describe the stiffness of polymers. At room temperature, $k_B T$ is $4.14 \times 10^{-21}$ J. For $A$, 0.38 nm was used.[20)]

Figure 2(a) shows a plot of $f$ against $z$ for the cases of $d = 0$, 5, 10, and 15 nm. Since the cantilever measures the force in the $z$ direction, $f_z$, the relationship between $f_z$ and $f$ in the direction along the molecular linker is

$$f_z = \frac{z}{\sqrt{z^2 + d^2}} f. \tag{2}$$

Figure 2(b) shows the relationship between $f$ and $f_z$ in the cases of $d = 0$, 5, 10, and 15 nm. When $d$ is nonzero, $f$ has a nonzero value even when $f_z = 0$. This is due to that fact that the molecular linker is elongated from the start of measurement when $d$ is nonzero. Even the case of $d = 5$ nm, the discrepancy between $f_z$, and $f$ was ~3 pN.

According to the Bell–Evans model,[4,12,13)] the rupture rate $k$ (rupture probability per unit time) under force $f$ can be written as

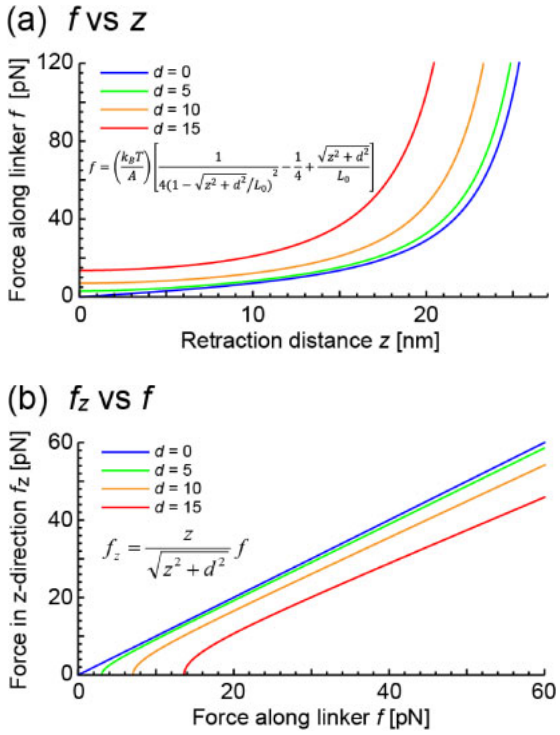


**Fig. 2.** (Color online) Force along (a) molecular linker $f$ and (b) $z$-direction $f_z$, which are indicated in Fig. 1(b).

$$k = k_0 \exp\left(\frac{x_b f}{k_B T}\right). \tag{3}$$

Thus, the differential equation for $S$, the probability that two molecules coupled at $t = 0$ remain coupled at $t = t$, and its solution are written in terms of $k$ as

$$\frac{dS(t)}{dt} = -k(t)S(t), \tag{4}$$

$$S(t) = S(0)\exp\left[-\int_0^t k(t')\,dt'\right] = \exp\left[-\int_0^t k(t')\,dt'\right], \tag{5}$$

where $S(0) = 1$ was used. Since the loading rate is constant ($r = r_c$) and feedback is applied to the measured force $f_z$, then $f_z$ can be written as,

$$f_z = \frac{z}{\sqrt{z^2 + d^2}} f = r_c t. \tag{6}$$

Therefore, the distribution of the rupture force $f_z$ can be written as

$$kS(t) = kS(f_z). \tag{7}$$

Then, the modal rupture force $f_z^*$ that gives the maximum value of $kS(t)$ is expressed as

$$f_z^* = \frac{k_B T}{x_b} \ln r_c + \frac{k_B T}{x_b} \ln\left(\frac{x_b \tau_{off}^d}{k_B T}\right), \tag{8}$$

where $\tau_{off}^d$ is the lifetime under the condition of $f_z = 0$ ($f \neq 0$ if $d$ is nonzero) and is given by

$$\tau_{off}^d = \left(\frac{1}{k}\right)_{f_z = 0}. \tag{9}$$

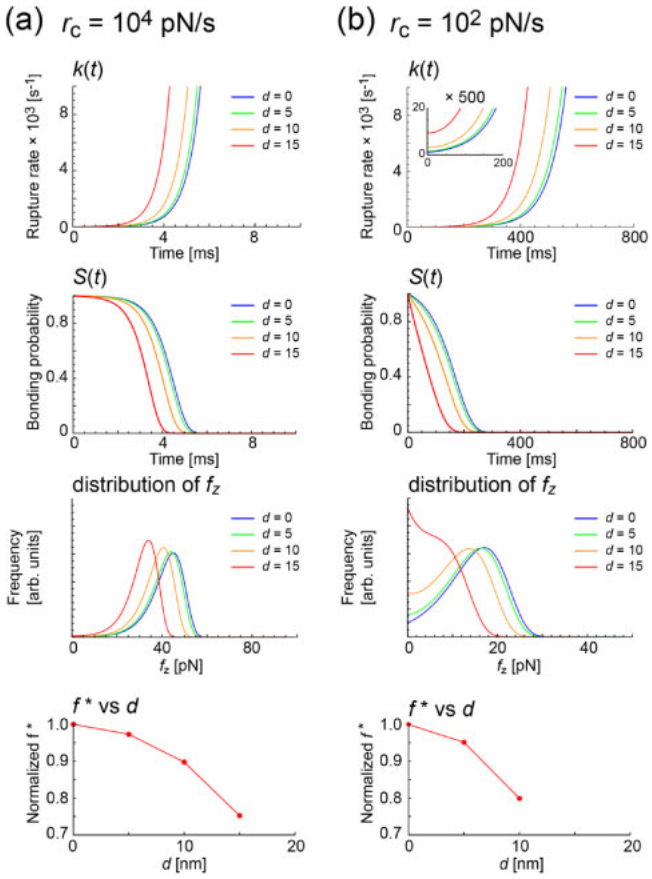


**Fig. 3.** (Color online) Rupture rate $k(t)$ and bonding probability $S(t)$ as a function of time, and rupture force distribution and normalized $f^*$ as a function of $d$ for (a) $r_c = 10^4$ pN/s and (b) $r_c = 10^2$ pN/s.

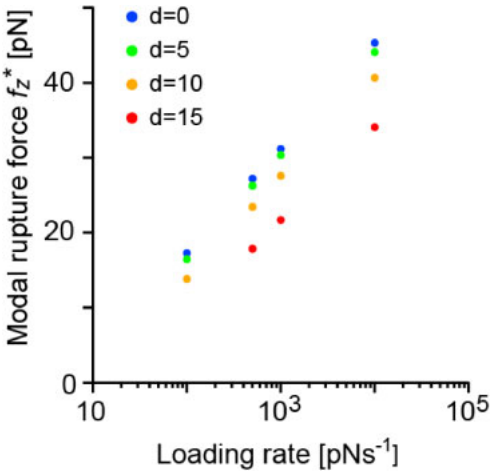


**Fig. 4.** (Color online) $f^*$ as a function of $r_c$ for $L = 30$ nm obtained by simulation.

**Table I.** Values obtained from Fig. 4.

| $d$ (nm) | $\tau_{off}^d$ (s) | $x_b$ (nm) |
|---|---|---|
| 0 | 1.0 | 0.68 |
| 5 | 0.94 | 0.69 |
| 10 | 0.64 | 0.71 |
| 15 | 0.30 | 0.77 |

Using Eqs. (3), (5), and (7) with the values of $x_b = 0.68$ nm, $k_0 = 1\ s^{-1}$, $T = 300$ K, and the spring constant of the cantilever of 6 pN/nm, which were used for the experiment schematically shown in Fig. 1(e), $k$, $S(t)$, and the distribution of the rupture force were calculated and the results are shown in Fig. 3 for (a) $r_c = 10^4$ pN/s and (b) $r_c = 10^2$ pN/s. For $r_c = 10^4$ pN/s, the values of $f_z^*$ were estimated to be 45.3, 44.1, 40.7, and 34.1 pN for $d = 0$, 5, 10, and 15 nm, while for $r_c = 10^2$ pN/s, $f_z^*$ was 17.3, 16.5, and 13.8 pN for $d = 0$, 5, and 10 nm, respectively. The distribution function for $d = 15$ nm was distorted for $r_c = 10^2$ pN/s, indicating that rupture occurred from the start of the measurement, as discussed above for the relation between $f$ and $f_z^*$. In the case of $d = 20$ nm (not shown), the distribution function was distorted even for $r_c = 10^3$ pN/s. These results suggest that the analysis can be carried out provided $d \lesssim 15$ nm. The normalized $f_z^*$ is summarized as a function of $d$ in the bottom of Fig. 3; $f_z^*$ decreases with increasing $d$.

## 3. Results and discussion

Next, we examined how a molecular linker affects the accuracy of the obtained $x_b$ and $\tau$. Figure 4 shows the relationship between $f_z^*$ and the logarithm of $r_c$ for $L_0 = 30$ nm, which is given by Eq. (8). First, a linear relationship remains even when $d$ is nonzero. Secondly, the slopes observed experimentally were similar for different values of $d$. From the reciprocal value of the slope of the straight line and its intercept, as explained using Fig. 1(d), $x_b$ and $\tau_{off}$ were obtained, respectively, which are summarized in Table I. $x_b$ increases with increasing $d$, and the increase in $x_b$ from its value when $d = 0$ was ~5% for $d = 10$ nm and ~10% for $d = 15$ nm. These values are sufficiently small to ensure the validity of DFS analysis.

On the other hand, $\tau$ decreased with increasing $d$, whose effect was larger than that on $x_b$. The reduction in $\tau$ from its value when $d = 0$ was ~35% for $d = 10$ nm and ~70% for $d = 15$ nm. This is due to the change in the intercept caused by the change in the slope having a greater effect. Values of $\tau$ have been scattered over four orders of magnitude in past works.[7,11] Here, it has been clearly shown that the molecular linker does not cause such large scattering, which is therefore considered to be caused by factors such as the method of fixing the sample molecule to the substrate, the pH of the solvent,[8,10,11] and the modification of the energy landscape, which cannot be simply treated by the Bell–Evans model.[21,22] The lifetime, which is determined by the potential height, is sensitive to changes in the potential landscape because the rupture rate $k$ has the exponential form shown in Eq. (3). These factors should be investigated by DFS with detailed theoretical analysis. As has been shown, when $d$ is nonzero and the atomic force microscope cantilever is retracted, a force $f$ is applied to the coupled molecule at the angle of $\theta = \arctan(z/d)$. Therefore, two-dimensional mapping of the force, which provides the relationship between $d$ and $f_z^*$, and thus $\theta$ and $f_z^*$, may give more detailed information on such interactions at local sites. This issue is left for future work.

Similar calculations can be carried out for different $L_0$ because Eq. (1) has the single parameter of $L/L_0$ for the molecular linker. For example, for $L_0 = 90$ nm, $d = 0$, 15, 30, and 45 nm give the same values of $f_z^*$ as those obtained for $L_0 = 30$ nm with $d = 0$, 5, 10, and 15 nm, respectively. Therefore, $L_0$ cannot be theoretically optimized. However,

when the molecular linker does not have a sufficient length, since the effects of the cantilever apex and the size of the receptor cannot be neglected, the use of a relatively long molecular linker is considered to produce a better measurement condition. On the other hand, for a long $L_0$, a coupling may also be formed at neighboring sites with different values of $d$, depending on the density of molecules on the substrate surface. Therefore, $L_0$ should be chosen in consideration of the measurement conditions.

## 4. Conclusion

We examined the effect of the molecular linker used to fix the target molecule to the atomic force microscope cantilever used in DFS, i.e., the force direction during measurement, for the first time, which has not been discussed until now despite its importance. The effect was found to be small, confirming the high potential of DFS. Further advances in the DFS technique are expected to enable more detailed analysis of the molecular interactions at the single-molecule level.

## Acknowledgment

H.S. acknowledges the support from the Japan Society for the Promotion of Science through Grant-in-Aid for Scientific Research, 15H05734.

1) T. A. Sulchek, R. W. Friddle, K. Langry, E. Y. Lau, H. Albrecht, T. V. Ratto, S. J. DeNardo, M. E. Colvin, and A. Noy, Proc. Natl. Acad. Sci. U.S.A. **102**, 16638 (2005).
2) G. Neuert, C. Albrecht, E. Pamir, and H. E. Gaub, FEBS Lett. **580**, 505 (2006).
3) D. Alsteens, M. Pfreundschuh, C. Zhang, P. M. Spoerri, S. R. Coughlin, B. K. Kobilka, and D. J. Muller, Nat. Methods **12**, 845 (2015).
4) R. Merkel, P. Nassoy, A. Leung, K. Ritchie, and E. Evans, Nature **397**, 50 (1999).
5) C. B. Yuan, A. Chen, P. Kolb, and V. T. Moy, Biochemistry **39**, 10219 (2000).
6) A. B. Patel, S. Allen, M. C. Davies, C. J. Roberts, S. J. B. Tendler, and P. M. Williams, J. Am. Chem. Soc. **126**, 1318 (2004).
7) M. D. Piramowicz, P. Czuba, M. Targosz, K. Burda, and M. Szymonski, Acta Biochim. Pol. **53**, 93 (2006).
8) A. Taninaka, O. Takeuchi, and H. Shigekawa, Appl. Phys. Express **2**, 085002 (2009).
9) O. Takeuchi, T. Miyakoshi, A. Taninaka, K. Tanaka, D. Cho, M. Fujita, S. Yasuda, S. P. Jarvis, and H. Shigekawa, J. Appl. Phys. **100**, 074315 (2006).
10) A. Taninaka, O. Takeuchi, and H. Shigekawa, Phys. Chem. Chem. Phys. **12**, 12578 (2010).
11) A. Taninaka, O. Takeuchi, and H. Shigekawa, Int. J. Mol. Sci. **11**, 2134 (2010).
12) E. Evans, Faraday Discuss. **111**, 1 (1999).
13) G. Bell, Science **200**, 618 (1978).
14) J. Wong, A. Chilkoti, and V. T. Moy, Biomol. Eng. **16**, 45 (1999).
15) F. Pincet and J. Husson, Biophys. J. **89**, 4374 (2005).
16) S. S. Andrews, Phys. Biol. **11**, 011001 (2014).
17) M. D. Wang, H. Yin, R. Landick, J. Gelles, and S. M. Block, Biophys. J. **72**, 1335 (1997).
18) C. Bouchiat, M. D. Wang, J. F. Allemand, T. Strick, S. M. Block, and V. Croquette, Biophys. J. **76**, 409 (1999).
19) Y. Chan, R. G. Haverkamp, and J. M. Hill, J. Theor. Biol. **262**, 498 (2010).
20) F. Kienberger, V. P. Pastushenko, G. Kada, H. J. Gruber, C. Riener, H. Schindler, and P. Hinterdorfer, Single Mol. **1**, 123 (2000).
21) J. Husson and F. Pincet, Phys. Rev. E **77**, 026108 (2008).
22) O. Björnham and S. Schedin, Eur. Biophys. J. **38**, 911 (2009).